

# STEEL participates in fracture healing through upregulating angiogenesis-related genes by recruiting PARP 1

S.-Z. ZHANG, Z.-F. LU, Y.-J. XU, H.-F. SHI, Y.-Z. LIU, Y.-J. RUI

Department of Hand Surgery, Wuxi Nine Hospital Affiliated to Soochow University, Wuxi, China

**Abstract. – OBJECTIVE:** To explore the effect of STEEL on fracture healing and its underlying mechanism.

**PATIENTS AND METHODS:** A total of 31 patients with long bone fracture and who received reoperation because of bone nonunion, delayed union or healing disorder in the Wuxi Nine Hospital Affiliated to Soochow University from July 2016 to February 2018 were selected. The bone callus at the fracture site was collected from each patient during the reoperation. QRT-PCR (Quantitative Real-Time Polymerase Chain Reaction) was used to detect STEEL expression in the callus tissues of the treatment group (bone nonunion or delayed union) and the control group. In addition, we measured the number of blood vessels in the fracture tissues by immunohistochemistry. After the construction of tibial fracture model in mice, STEEL expression and the total number of blood vessels in the treatment group (sawing treatment) and the control group (sham operation) were detected, respectively. For *in vitro* experiments, CCK-8 (cell counting kit-8) assay was performed to detect cell proliferation after knockdown or overexpression of STEEL in the vascular endothelial cells. The binding condition of STEEL and its interacting proteins were detected by RIP (RNA binding protein immunoprecipitation), and the binding of PARP 1 [poly (ADP-ribose) polymerase 1] with gene promoter was observed by ChIP (chromatin immunoprecipitation assay). Western blot was used to detect the expression level of VEGF (vascular endothelial growth factor).

**RESULTS:** STEEL expression and the vascular density in the callus tissues of the treatment group were significantly lower than those of the control group. Downregulated STEEL remarkably decreased the proliferation ability of HUVEC cells. Meanwhile, the vascular density was also significantly decreased in mice with a tibial fracture. Overexpressed STEEL obtained the opposite results. STEEL could interact with PARP 1 to regulate expressions of downstream genes. Moreover, STEEL could also promote angiogenesis by elevating VEGF expression.

**CONCLUSIONS:** We showed that STEEL expression could partly represent the angiogenesis of fracture sites. Moreover, it promoted angiogenesis by elevating VEGF expression.

*Key Words:*

Fracture healing, Long non-coding RNA, Vascular endothelium, PARP 1.

## Introduction

Fracture healing is a tissue repair reaction between the broken ends of the fracture. During the process of fracture healing, fractured bone can be completely replaced by new bones with the original structure and function<sup>1</sup>. It is reported that the incidence of bone nonunion and delayed union is about 8-10% in China<sup>2</sup>. In recent years, the United States Health System Statistics showed that there are about 5 million cases with different sites and different types of bone fracture in the United States annually<sup>3</sup>. At present, the underlying mechanism of fracture healing is still unclear<sup>4</sup>. As fracture healing is a continuous process with the balance of destruction and regeneration, the natural healing process of fracture can be divided into three stages. However, there is a close relationship between each stage, which cannot be completely separated. Meanwhile, the internal and external environment of the body, including blood circulation, nutrition<sup>5</sup>, and external mechanics<sup>6</sup> may exert invaluable roles in this process<sup>7,8</sup>. Therefore, maintenance of a good local blood supply in the fracture site is of great significance in the treatment of the fracture.

Long non-coding RNAs (lncRNAs) are a class of RNAs with over 200 nucleotides (nt) in length. LncRNA does not or rarely participate in coding proteins<sup>9</sup>. In mammals, lncRNA is mainly transcribed by RNA polymerase II or III. Howe-

ver, it is transcribed by RNA polymerase IV and V in plants<sup>10</sup>. In general, lncRNA is divided into 5 categories, including sense, antisense, bidirectional, intronic and intergenic lncRNA. There are a variety of sources of lncRNAs, including the five kinds as the follows: (1) Gene structure of the coding protein is interrupted and transformed into lncRNA; (2) The result of chromatin recombination, that is, two non-transcriptional genes are juxtaposed with another independent gene to produce lncRNAs containing multiple exons; (3) Reverse shift in the process of non-coding gene replication; (4) Generation of contiguous lncRNAs from local tandem replicator; (5) A functional non-coding RNA that is produced by insertion of transposable component into a gene<sup>11</sup>. Although the source of lncRNAs varies, studies have shown that they exhibit a similar role in the regulation of gene expressions. lncRNA participates in the regulatory process at the epigenetic, transcriptional and post-transcriptional levels, which exerts a crucial role in multiple life activities including fracture healing<sup>12,13</sup>. This study aims to explore the role of lncRNA STEEL in fracture healing and its underlying mechanism<sup>14</sup>.

## Patients and Methods

### Research Subjects and Tissue Specimen

A total of 31 patients with long bone fracture and who received reoperation because of bone non-union, delayed union or healing disorder in the Wuxi Nine Hospital Affiliated to Soochow University from July 2016 to February 2018 were selected. The average age of the patients was  $56.3 \pm 14.8$  years. The bone callus at the fracture site was collected from each patient during the reoperation. This study was approved by the Medical Ethics Committee of the Wuxi Nine Hospital Affiliated to Soochow University. Informed consent was obtained from each patient before specimen collection.

### Construction of the Fracture Model in Mice

1% sodium pentobarbital (1 mL/kg) was intraperitoneally injected to 36 male SD (Model Animal Research Center of Nanjing University, Nanjing, China) mice (6-8 weeks, 16.8-25.3 g) for anesthesia. No significant differences in the age, sex, and body weight of mice were found. Subsequently, the sham operation was performed on the left tibia of the mice. The right tibial diaphysis was treated with sawing to induce stable fracture, and the intrame-

dullary fixation needle was inserted and matched completely. The left tibia of mice was used as the control group (CG), while the tibial fracture healing model after the right fracture fixation was used as the treatment group (TG). The tissue engineering method was used to evaluate the *in vivo* role of STEEL in angiogenesis. The collagen model embedded in adipose mesenchymal stromal cells was embedded with transfected HUVEC cells and implanted into mice with deficient immunity. After implantation for 21 days, the density of blood vessel was measured by the animal living imaging system (CD31 was used as a marker of vascular endothelial cells in immune-histochemical staining). Images showed the development of the internal vascular network in the implanted collagen module and the implanted vascular system.

### Cell Culture

The vascular endothelial cell line (HUVEC) was provided by the American Type Collection Center (ATCC, Manassas, VA, USA) and cultured in completed DMEM (Dulbecco's Modified Eagle Medium) medium (Gibco, Grand Island, NY, USA), supplemented with 10% fetal bovine serum (FBS, Gibco, Grand Island, NY, USA). The cells were maintained in a 5% CO<sub>2</sub> incubator at 37°C. Cells were passaged when cell confluence was up to 80-90%.

### Cell Transfection

The cells were seeded into the 6-well plates, and Lipofectamine 2000 (Entranster-R4000 for pcDNA, Thermo Fisher Scientific, Waltham, MA, USA) was used for transfection when the cell confluence was around 60%. Firstly, 500  $\mu$ L of serum-free suspension containing 10  $\mu$ L of Lipofectamine 2000 and 10  $\mu$ L of siRNA-STEEL (4  $\mu$ L of Entranster-R4000 and 2.68  $\mu$ g of pcDNA-CRNDE were used for pcDNA) was added, and then, 1.5 mL of DMEM was added for cell culture. For the control group, isodose Lipofectamine 2000 and siRNA-NC (Entranster-R4000 and pcDNA-NC for pcDNA) were added. The culture medium was replaced 6 h after transfection. Sequences of siRNAs used in this study were: siRNA-STEEL: 5'-TGCCAAGCTGAGCAC-GTC-3', 5'-GCCCGAACCATGAGCTCCT-3'.

### Quantitative Reverse Transcriptase-Polymerase Chain Reaction (qRT-PCR)

We used TRIzol kit (Invitrogen, Carlsbad, CA, USA) to extract total RNA of the tissues. The reverse transcriptional reaction was perfor-

med under the following conditions: Reverse transcription reaction at 50°C for 30 min, and denaturation of reverse transcriptase at 92°C for 3 min. The obtained complementary Deoxyribose Nucleic Acid (cDNA) was amplified by the following PCR amplification reaction conditions: Denaturation at 92°C for 10 s, annealing at 55°C for 20 s and extension at 68°C for 20 s, for a total of 40 cycles.  $\beta$ -action was used as the internal reference, and the relative expression of SNHG12 was represented by  $2^{-\Delta\Delta Ct}$ . Primers used in qRT-PCR were as follows:  $\beta$ -action: F: 5'-CTCCATCCTGGCCTCGCT-GT-3', R: 5'-GCTGTACCTTCACCGTTCC-3'; STEEL: F: 5'-TCACCAACCACGGACATTC-3', R: 5'-AGCCAAGTCAGACGAATAT-3'.

#### **Cell Counting Kit-8 (CCK-8) Assay**

Transfected cells were collected and seeded into the 96-well plates at a dose of  $5 \times 10^3$ /well, with 6 replicates in each group. After culturing for 6 h, the activity of the adherent cells was measured. Briefly, 20  $\mu$ L of a CCK-8 solution (Dojindo Laboratories, Kumamoto, Japan) was added to each well at 24, 48, 72, and 96 h, respectively. Cells were incubated at 37°C for 2-3 h in the dark. Absorbance (OD) values at the wavelength of 450 nm were detected by the microplate reader (Bio-Rad, Hercules, CA, USA). The blank control was only incubated with a CCK-8 solution and the culture medium without cells.

#### **RIP Assay**

The determination of RNA immunoprecipitation (RIP) was performed according to the instructions of the Magna RIP™ RNA-binding protein immunoprecipitation Kit (Millipore, Bedford, MA, USA). Cells at a density of 80-90% were collected, and the RIP lysis buffer was used for cell lysis. Next, cell extracts were incubated with RIP buffer containing magnetic beads which were bound with the human anti-PARP 1 [poly (ADP-ribose) polymerase 1] antibody (sc-8007, Santa Cruz Biotechnology, Santa Cruz, CA, USA) or negative control IgG. The samples were incubated with protease K for protein digestion, and then, the precipitated RNA was obtained. Finally, the purified RNA was used for qRT-PCR analysis.

#### **Chromatin Immunoprecipitation (ChIP) Assay**

Cells were digested with phosphate buffered saline (PBS) containing 0.1% trypsin and 0.1% collagenase. Cell lysis and streptavidin

bead-particle precipitation were prepared by the Bioruptor instrument (Diagenode SA, Liege, Belgium). QRT-PCR was used to identify and quantify the precipitated RNA, and the relative expression was represented by  $2^{-\Delta\Delta Ct}$ . Primers used in this study were: KLF2 exon1/intron1: F: 5'-ATCCTGCCGTCCTTCTC-3'; R: 5'-GCAGCCCACGTTCTACTAC-3'; KLF2 intron1/exon2: F: 5'-TCACGCCCATTCGCCCTGTC-3'; R: 5'-GCGCCCAGGCCATCCAG-3'; eNOS exon1/intron1: F: 5'-CCAGCGCCAGAACACAGGTAAG-3'; R: 5'-GCCCTCCGACTCAGCTACAA-3'; eNOS intron1/exon2: F: 5'-GAAACAAACCCTTCCTGATGAC-3'; R: 5'-TTCTTCACACGAGGGAAGTTG-3'; eNOS promoter(-166to-26): F: 5'-GTGGAGCTGAGGCTTTAGAGC-3'; R: 5'-TTTCCTTAGGAGAGGGAGGG-3'; KLF2 promoter(-84to+50): F: 5'-TTCCGCCGCCGCCGCTTTG-3'; R: 5'-GGACGCGGACGGGGACACC-3'.

#### **Statistical Analysis**

We used Statistical Product and Service Solutions (SPSS22.0, IBM Corp., Armonk, NY, USA) Software (Statistic Package for Social Science) for all statistical analysis and GraphPad Prism 6.0 (La Jolla, CA, USA) for image editing. The quantitative data were represented as mean  $\pm$  standard deviation ( $\bar{x} \pm s$ ). The *t*-test was used for continuous variables, and the  $\chi^2$ -test was applied for categorical variables.  $p < 0.05$  was considered statistically significant (\* $p < 0.05$ , \*\* $p < 0.01$ , \*\*\* $p < 0.001$ ).

## **Results**

### **STEEL Was Closely Related to Angiogenesis During the Process of Fracture Healing**

QRT-PCR results showed that STEEL expression in callus tissues of the TG group (bone nonunion or delayed healing,  $n=22$ ) was remarkably lower than that of the CG group ( $n=9$ ) (Figure 1A). Moreover, the immunohistochemical analysis indicated that the vascular density in callus tissues of the TG group was markedly lower than that of the CG group (Figure 1B). In the tibial fracture model, results demonstrated that STEEL expression and the density of micro-vessels in the CG group were remarkably lower compared with those of TG group (Figure 1C and 1D). These results suggested that STEEL could be served as an indicator of blood supply in fracture healing.

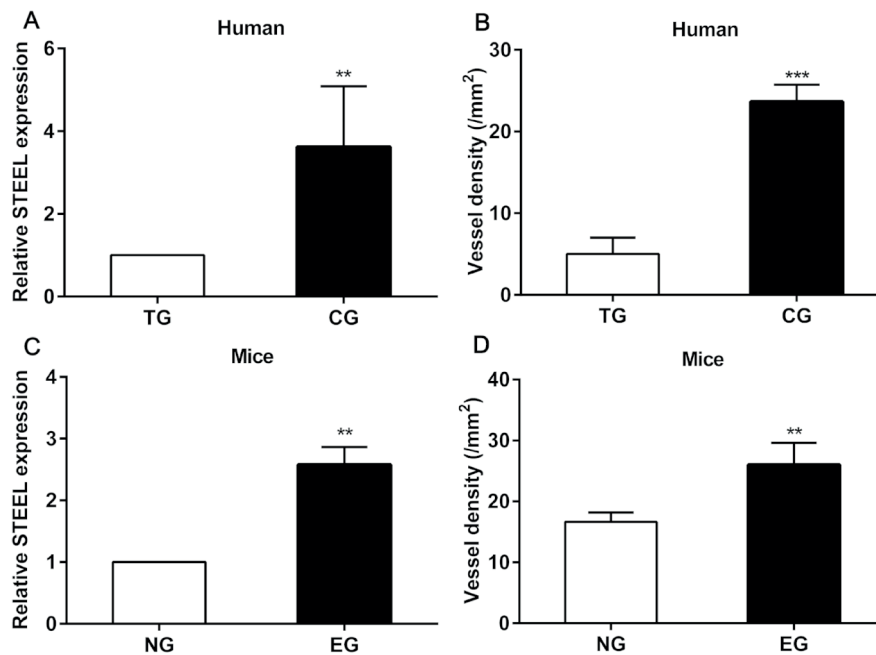


**Figure 1.** STEEL was associated with angiogenesis in the process of fracture healing. **A**, QRT-PCR results showed that the expression of STEEL in callus tissues of the TG group (n = 22) was significantly lower than that of the CG group (n=9); **B**, Immunohistochemistry indicated that the vascular density in callus tissues of the TG group was significantly lower than that of the CG group; **C**, QRT-PCR results demonstrated that, in the tibial fracture model, the expression of STEEL in the CG group were significantly lower than the TG group; **D**, Immunohistochemistry indicated, in the tibial fracture model, the vascular density in callus tissues of the TG group was significantly higher than the CG group.

### **STEEL Promoted the Proliferation of Vascular Endothelial Cells *In Vitro* and Angiogenesis *In Vivo***

To explore the effect of STEEL on angiogenesis, we first knocked down STEEL in vascular endothelial cells by transfecting a small interference RNA (Figure 2A). CCK-8 results indicated that the proliferation ability was remarkably decreased after si-STEEL transfection in HUVEC cells (Figure 2B). *In vivo* experiments also showed the reduced density of blood vessels formed by the transplanted HUVEC cells after transfection with si-STEEL (Figure 2C). Overexpressing STEEL in HUVEC cells obtained the opposite results (Figure 2D-2F). These results indicated that STEEL could enhance the proliferation of vascular endothelial cells *in vitro* and promote angiogenesis *in vivo*.

### **PARP 1 Could Interact With STEEL *In Vitro***

Recent studies have shown that PARP 1 and SNRNP70 can act as RNA binding partners, while some other proteins can interact with chromatin to influence gene expressions. In this study, we used RIP assay to detect the protein amounts

of PARP 1 and SNRNP70 combined with STEEL *in vitro* and results indicated that STEEL was significantly interacted with PARP 1 (Figure 3A). Related studies have demonstrated that lncRNAs can cooperate with proteins or locate regulatory proteins in genomic regions to regulate expressions of target genes. Therefore, we hypothesized that STEEL could recruit PARP 1 to the promoter region of target genes. Notably, CHIP results illustrated that the recruited PARP 1 to the KLF2 promoter region was remarkably reduced after si-STEEL transfection (Figure 3B). The above findings suggested that STEEL could interact with PARP 1 to promote its recruitment to target genes.

### **STEEL Affected the Expression of Angiogenesis-Related Gene**

Since STEEL exerted an important role in the process of angiogenesis *in vitro* and *in vivo*, we subsequently explored its effect on the expression of vascular endothelial growth factor (VEGF). Western blot results showed downregulated VEGF after STEEL knockdown in HUVEC cells (Figure 4A). Meanwhile, VEGF expression also exhibited a downward trend after PARP 1



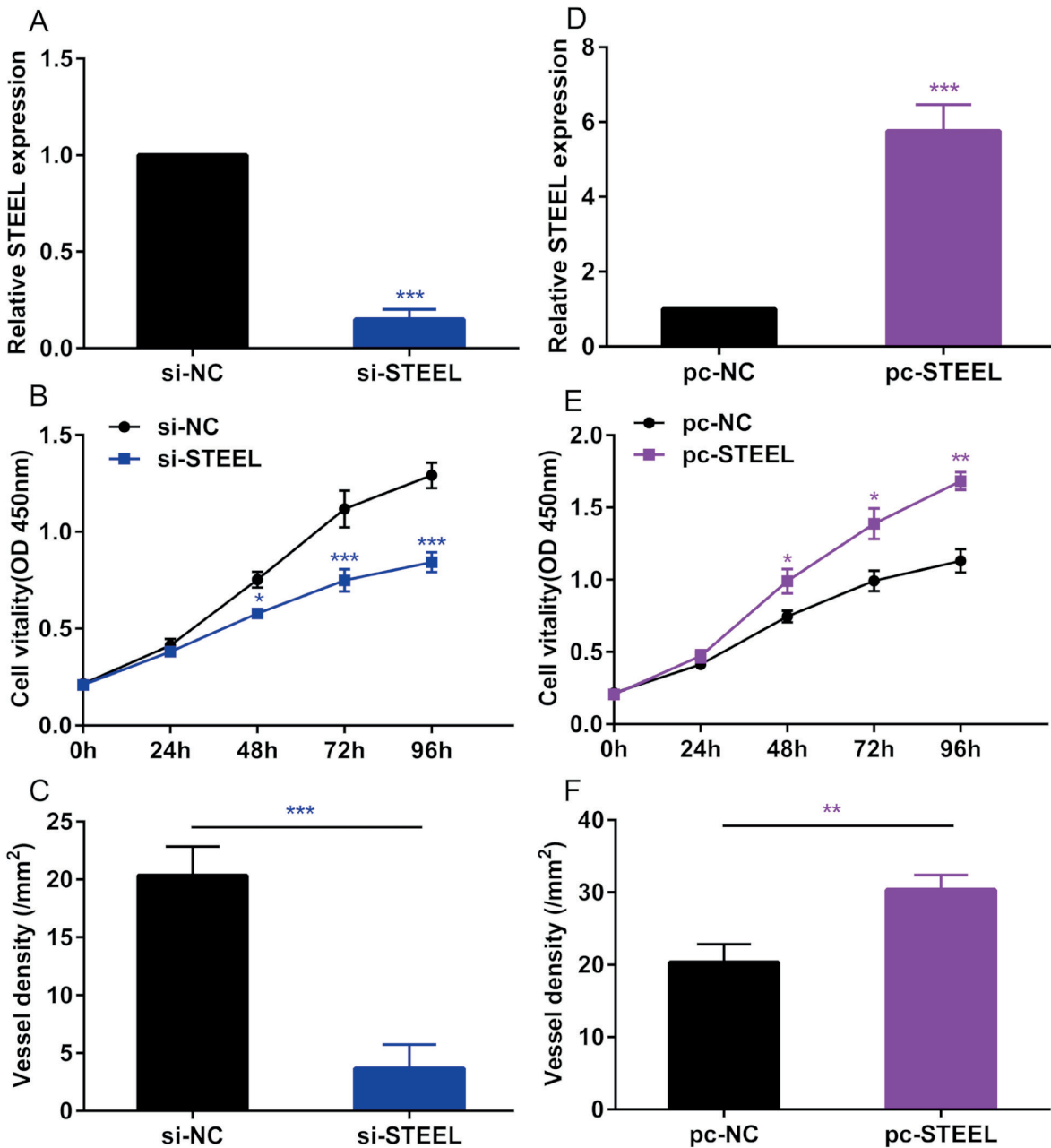


**Figure 2.** STEEL promoted the proliferation of vascular endothelial cells *in vitro* and angiogenesis *in vivo*. **A**, QRT-PCR results showed that, after Si-STEEL in HUVEC cells, the expression of STEEL was significantly decreased; **B**, CCK-8 results indicated that, after Si-STEEL in HUVEC cells, the proliferation ability was significantly decreased; **C**, After si-STEEL transfection in HUVEC cells, the vascular density of formed by transplants was significantly reduced; **D**, QRT-PCR results showed that, after overexpressing STEEL in HUVEC cells, the expression of STEEL was significantly increased; **E**, CCK-8 results indicated that, after overexpressing STEEL in HUVEC cells, the proliferation ability was significantly increased; **F**, After overexpressing STEEL in HUVEC cells, the vascular density of formed by transplants was significantly increased.

knockdown (Figure 4A). To further explore the relationship between STEEL and PARP 1, we detected PARP 1 expression in HUVEC cells transfected with si-STEEL. QRT-PCR results showed that the downregulated STEEL had no significant

effect on PARP 1 (Figure 4B). All the above results indicated STEEL might promote angiogenesis by interacting with PARP 1, affecting expressions of downstream genes and promoting VEGF expression.

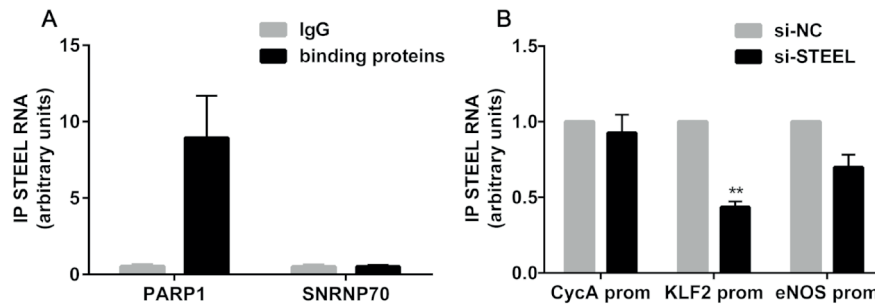


**Figure 3.** Synergistic effect of STEEL and PARP 1 on the promoter region of KLF2. **A**, RIP results showed that PARP 1 rather than SNRNP70 could interact with STEEL; **B**, CHIP results illustrated that the PARP 1 recruited to the KLF2 promoter region was significantly reduced after Si-STEEL, whereas there were no changes in the promoter region of CycA and eNOS.

## Discussion

Bone nonunion is a common complication of bone fracture, the incidence of which is about 5-10%. Clinical treatment of bone nonunion is a tough problem for clinicians<sup>15</sup>. In general, bone fracture can be healed within 3 months after fracture. Delayed healing is defined as healing for more than 3 months, and nonunion is defined as not healing after 6 months or no trend of healing for 3 months<sup>16</sup>. Although a prolonged treatment time may cure delayed healing, the long-term external fixation may eventually cause stiffness of limbs adjacent to joint and muscular disuse atrophy<sup>17,18</sup>. Therefore, establishing a good blood supply at the fracture site, curing bone nonunion as early as possible and recovering limb function have become urgent expectations for patients and doctors.

Only 1.5-2% of the protein-coding genes in the human genome can be transcribed steadily, and most of the remaining RNAs could not encode protein. LncRNAs are a class of heterogeneous

non-coding RNAs. According to different functions of lncRNAs, they are divided into signal molecules, bait molecules, guiding molecules, and skeleton molecules. LncRNAs were initially considered as by-products during the evolution process. With in-depth researches, lncRNA has been well recognized as its biological function<sup>19</sup>. More and more studies have shown that proximal promoter sequences, exons, introns, and second-level structures of lncRNAs are highly conserved<sup>20</sup>, which can regulate gene expression at epigenetic, transcriptional and post-transcriptional levels<sup>21</sup>. Additionally, several researches have indicated that lncRNA is associated with a variety of human physiological and pathological processes<sup>22</sup>.

Our study identified the relationship between STEEL and angiogenesis by detecting STEEL expression and vascular density in human callus tissues. *In vitro* functional experiments showed that STEEL could significantly promote the proliferation of vascular endothelial cells. By constructing a tibial fracture model in mice, we also verified the effect of STEEL on angiogenesis

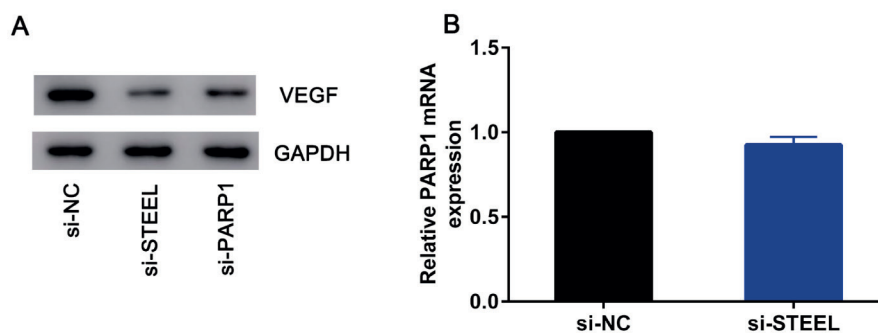


**Figure 4.** Synergistic effect of STEEL and PARP 1. **A**, Western blot results showed that, after knocking down the expression of STEEL or PARP 1 in HUVEC cells, the protein expression of VEGF decreased significantly; **B**, After si-STEEL transfection in HUVEC cells, there was no obvious change of the expression of PARP 1.

*in vivo*. In addition, STEEL could interact with PARP 1 to remarkably increase its recruitment by the KLF2 promoter region and promote VEGF expression, thereby contributing to angiogenesis in fracture healing.

## Conclusions

STEEL could be served as a potential indicator of angiogenesis at the fracture site. Moreover, STEEL regulated expressions of downstream genes by interacting with PARP 1 and promoted angiogenesis by upregulating VEGF.

## Conflict of Interest

The Authors declare that they have no conflict of interest.

## References

- 1) SU B, SHENG H, ZHANG M, BU L, YANG P, LI L, LI F, SHENG C, HAN Y, QU S, WANG J. Risk of bone fractures associated with glucagon-like peptide-1 receptor agonists' treatment: a meta-analysis of randomized controlled trials. *Endocrine* 2015; 48: 107-115.
- 2) MEESTERS DM, NEUBERT S, WUNANDS K, HEYER FL, ZEITER S, ITO K, BRINK P, POEZE M. Deficiency of inducible and endothelial nitric oxide synthase results in diminished bone formation and delayed union and nonunion development. *Bone* 2016; 83: 111-118.
- 3) SANTOLINI E, WEST R, GIANNI P. Risk factors for long bone fracture non-union: a stratification approach based on the level of the existing scientific evidence. *Injury* 2015; 46 Suppl 8: S8-S19.
- 4) HE X, MENG Y, HUANG Y, HAO D, WU Q, LIU J. Factors affecting delayed union of vertebral fractures following percutaneous kyphoplasty. *Pain Physician* 2017; 20: E241-E249.
- 5) HEIKKILA K, PEARCE J, MAKI M, KAUKINEN K. Celiac disease and bone fractures: a systematic review and meta-analysis. *J Clin Endocrinol Metab* 2015; 100: 25-34.
- 6) GARG RK, AFIFI AM, GASSNER J, HARTMAN MJ, LEVERSON G, KING TW, BENTZ ML, GENTRY LR. A novel classification of frontal bone fractures: the prognostic significance of vertical fracture trajectory and skull base extension. *J Plast Reconstr Aesthet Surg* 2015; 68: 645-653.
- 7) FROTZLER A, COUPAUD S, PERRET C, KAKEBEEKE TH, HUNT KJ, DONALDSON NN, ESER P. High-volume FES-cycling partially reverses bone loss in people with chronic spinal cord injury. *Bone* 2008; 43: 169-176.
- 8) LIU B, XIONG Y, DENG H, GU S, JIA F, LI Q, WANG D, GAN X, LIU W. Comparison of our self-designed rotary self-locking intramedullary nail and interlocking intramedullary nail in the treatment of long bone fractures. *J Orthop Surg Res* 2014; 9: 47.
- 9) RUIZ-ORERA J, MESSEGUER X, SUBIRANA JA, ALBA MM. Long non-coding RNAs as a source of new peptides. *eLife* 2014; 3: e3523.
- 10) MALLORY AC, SHKUMATAVA A. LncRNAs in vertebrates: advances and challenges. *Biochimie* 2015; 117: 3-14.
- 11) KELLER C, BUHLER M. Chromatin-associated ncRNA activities. *Chromosome Res* 2013; 21: 627-641.
- 12) SUN C, LIU X, YI Z, XIAO X, YANG M, HU G, LIU H, LIAO L, HUANG F. Genome-wide analysis of long non-coding RNA expression profiles in patients with non-alcoholic fatty liver disease. *IUBMB Life* 2015; 67: 847-852.
- 13) WANG XN, ZHANG LH, CUI XD, WANG MX, ZHANG GY, YU PL. LncRNA HOXA11-AS is involved in fracture healing through regulating mir-124-3p. *Eur Rev Med Pharmacol Sci* 2017; 21: 4771-4776.
- 14) MAN HSJ, SUKUMAR AN, LAM GC, TURGEON PJ, YAN MS, KU KH, DUBINSKY MK, HO JJD, WANG JJ, DAS S, MITCHELL N, OETTGEN P, SEFTON MV, MARSDEN PA. Angiogenic patterning by STEEL, an endothelial-enriched long noncoding RNA. *Proc Natl Acad Sci U S A* 2018; 115: 2401-2406.
- 15) MONTAVA M, MANCINI J, MASSON C, COLLIN M, CHAUMOTRE K, LAVIEILLE JP. Temporal bone fractures: sequelae and their impact on quality of life. *Am J Otolaryngol* 2015; 36: 364-370.
- 16) BAKER R, ORTON E, TATA LJ, KENDRICK D. Risk factors for long-bone fractures in children up to 5 years of age: a nested case-control study. *Arch Dis Child* 2015; 100: 432-437.
- 17) KANG HM, KIM MG, HONG SM, LEE HY, KIM TH, YEO SG. Comparison of temporal bone fractures in children and adults. *Acta Otolaryngol* 2013; 133: 469-474.
- 18) TASSANI S, MATSOPOULOS GK. The micro-structure of bone trabecular fracture: an inter-site study. *Bone* 2014; 60: 78-86.
- 19) VOLDERS PJ, HELSENS K, WANG X, MENTEN B, MARTENS L, GEVAERT K, VANDESOMPELE J, MESTDAGH P. LNCipedia: a database for annotated human lncRNA transcript sequences and structures. *Nucleic Acids Res* 2013; 41: D246-D251.
- 20) MERCER TR, MATTICK JS. Structure and function of long noncoding RNAs in epigenetic regulation. *Nat Struct Mol Biol* 2013; 20: 300-307.
- 21) BOHMDORFER G, WIERZBICKI AT. Control of chromatin structure by long noncoding RNA. *Trends Cell Biol* 2015; 25: 623-632.
- 22) KAZEMZADEH M, SAFARALIZADEH R, ORANG AV. LncRNAs: emerging players in gene regulation and disease pathogenesis. *J Genet* 2015; 94: 771-784.